Ultrafast Dynamics of Encapsulated Molecules Reveals New Insight on the Photoisomerization Mechanism for Azobenzenes

Christopher J. Otolski,[†] A. Mohan Raj,[‡] Vaidhyanathan Ramamurthy,[*,‡] and Christopher G. Elles[*,†]

[†]*Department of Chemistry, University of Kansas, Lawrence, KS 66045, United States*

[‡]*Department of Chemistry, University of Miami, Coral Gables, FL 33146, United States*

E-mail: murthy1@miami.edu; elles@ku.edu

Abstract

Spatial confinement can have a profound impact on the dynamics of chemical reactions, especially for isomerization reactions that involve large amplitude structural rearrangement of a molecule. This work uses ultrafast spectroscopy to probe the effects of confinement on *trans*→*cis* photoisomerization following $\pi\pi^*$ excitation of 4-propyl stilbene and 4-propyl azobenzene encapsulated in a supramolecular host-guest complex. Transient absorption spectroscopy of the encapsulated azobenzene derivative reveals the formation of two distinct excited-state species with spectral signatures resembling the *cis* and *trans* isomers. Formation of the *cis* species indicates a direct excited-state isomerization channel that is not observed in cyclohexane solution. Comparison with the stilbene analogue suggests that this "hot" excited-state isomerization pathway for encapsulated azobenzene involves primarily in-plane inversion, whereas a ten-fold increase of the excited-state lifetime for the *trans* isomer suggests that crowding in the capsule hinders isomerization from the relaxed S_1 geometry of the *trans* isomer. This work provides new mechanistic insight on the relative roles of inversion and rotation in the ultrafast photoisomerization of azobenzene derivatives.

Graphical TOC Entry

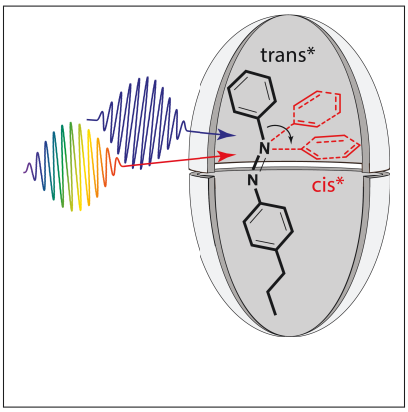

Nature makes use of steric constraints to guide the early stages of many light-activated biological responses.[1] For example, many light-sensitive biological functions, including vision and phototaxy, begin with *cis-trans* photoisomerization in the spatially confined active site of a protein, where steric and other interactions determine the ultrafast reaction dynamics.[2–5] Similar to the way some proteins drive isomerization around a specific C=C or N=N double bond of a chromophore, synthetic cavities present an opportunity to selectively manipulate the dynamics of photochemical reactions by influencing the structural rearrangement of a molecule,[6–13] or even pre-aligning the reactants in a bimolecular reaction.[14,15] Reactions in confined environments not only open the possibility of new applications, but also provide a window on the underlying details that control the reaction dynamics.[16]

In this letter, we use ultrafast spectroscopy to study the influence of a restricted environment on the *trans*→*cis* photoisomerization dynamics of 4-propyl stilbene (4PrSt) and 4-propyl azobenzene (4PrAz) encapsulated in a supramolecular organic capsule.[10] Stilbene and azobenzene derivatives are prototypical photochromic compounds that are ubiquitous in applications where environmental effects could alter the reaction dynamics, including biological triggers and probes,[17–22] molecular machines,[23,24] and photochromic materials.[25–28] Photoisomerization reactions are particularly sensitive to steric constraints, due to the large amplitude motions required for structural rearrangement. While the photoisomerization mechanism for stilbene derivatives requires out-of-plane rotation of the phenyl rings around the central C=C double bond, the mechanism for azobenzene is complicated by possible contributions from both rotation and in-plane inversion pathways.[29,30] We show below that confining these molecules within an appropriately sized cavity provides a window on the isomerization mechanism by restricting the rotation of the phenyl rings around the double bond. We observe a bifurcation between *cis* and *trans* isomers in the excited state of azobenzene that indicates a new excited-state inversion pathway that is not observed in solution.

The host-guest complexes that we study spontaneously self-assemble in aqueous solution by incarcerating a single stilbene or azobenzene molecule in the hydrophobic cavity formed

by two cavitand molecules. The synthesis of the cavitand molecule, known as octa-acid (OA), and the preparation of OA_2 dimer complexes encapsulating a hydrophobic chromophore were reported elsewhere, along with detailed studies of the photochemistry inside the capsules based on steady-state measurements.[10,31–35] Stilbene and azobenzene derivatives are known to isomerize in the OA_2 capsules,[31–33] but the ultrafast excited-state dynamics have not been studied previously. In this study, we use propyl-substituted stilbene and azobenzene, because the inert alkyl chain causes additional crowding inside the capsule, and therefore exacerbates the effects of the confined environment. We note that alkyl-substituted stilbene and azobenzene have essentially the same isomerization mechanisms as the unsubstituted counterparts in solution. However, unlike solution, the *cis* isomers are the more stable structure in the capsule because crowding disproportionately destabilizes the longer *trans* isomers.[32]

The chemical structure of OA is shown as an inset in the top panel of figure 1, along with the absorption spectrum of the OA_2 dimer capsule formed by encapsulating an optically transparent and chemically inert adamantane molecule. The lower two panels of the figure show the spectra of encapsulated *trans*-4PrSt and *trans*-4PrAz, respectively, as well as the spectra of the two chromophores dissolved in cyclohexane. The absorption band of OA is centered near 280 nm, and partially overlaps the ground-state absorption of 4PrSt and 4PrAz. The absorption spectra of both compounds become slightly broader and have less vibronic structure upon encapsulation, suggesting that both molecules are distorted in the capsule. Molecular dynamics calculations for encapsulated *trans*-stilbene derivatives indicate a slightly twisted structure in the ground state, compared with a planar ground state in solution (see figure S2 in the supplemental information, SI).

Figure 2 shows the evolution of the transient absorption (TA) spectra following $\pi \rightarrow \pi^*$ excitation of 4PrSt and 4PrAz at 320 nm, where there is no absorption by the OA_2 capsule. The figure shows the evolution of the TA spectra in cyclohexane (upper panels) and inside the capsule (middle panels), with the lower panels comparing the decay of the excited-state

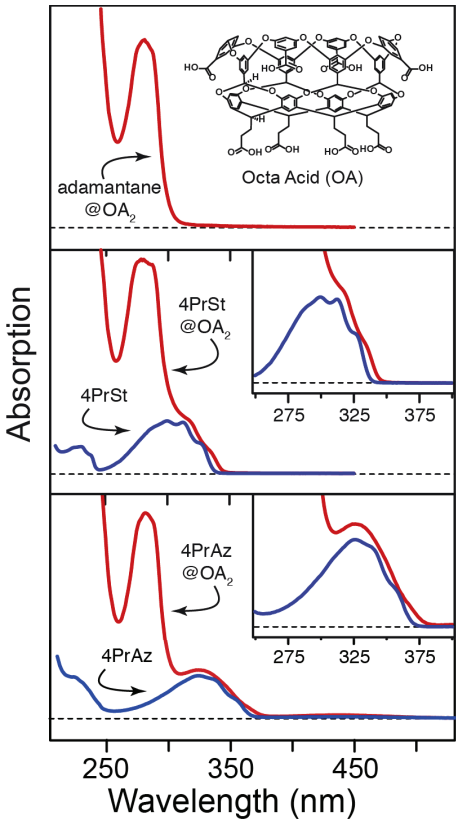

Figure 1: Absorption spectra of octa-acid complexes: adamantane@OA_2 (top), 4PrSt@OA_2 (middle), and 4PrAz@OA_2 (bottom). Lower panels also show the spectra of 4PrSt and 4PrAz in cyclohexane.

absorption bands as a function of time for each environment. Notice the different timescales for the two compounds.

The figure shows the isotropic TA spectra that we calculate from separate measurements with parallel and perpendicular polarization of the pump and probe light, $\Delta A_{iso} = (\Delta A_{||} + 2\Delta A_{\perp})/3$, in order to eliminate contributions from rotational reorientation. From the same set of measurements, we also calculate the anisotropy, $r(t) = (\Delta A_{||} - \Delta A_{\perp})/(\Delta A_{||} + 2\Delta A_{\perp})$, which provides a measure of the reorientation time for molecules in the excited state. The decay of the anisotropy reveals significantly slower reorientation in the capsules compared with solution (figure S8 in the SI), with the entire complex rotating on a ∼ns timescale, compared with tens of ps for the freely solvated molecules. Slower reorientation confirms that 4PrSt and 4PrAz are incarcerated in the OA_2 capsule, and that they do not rotate

inside the cavity.

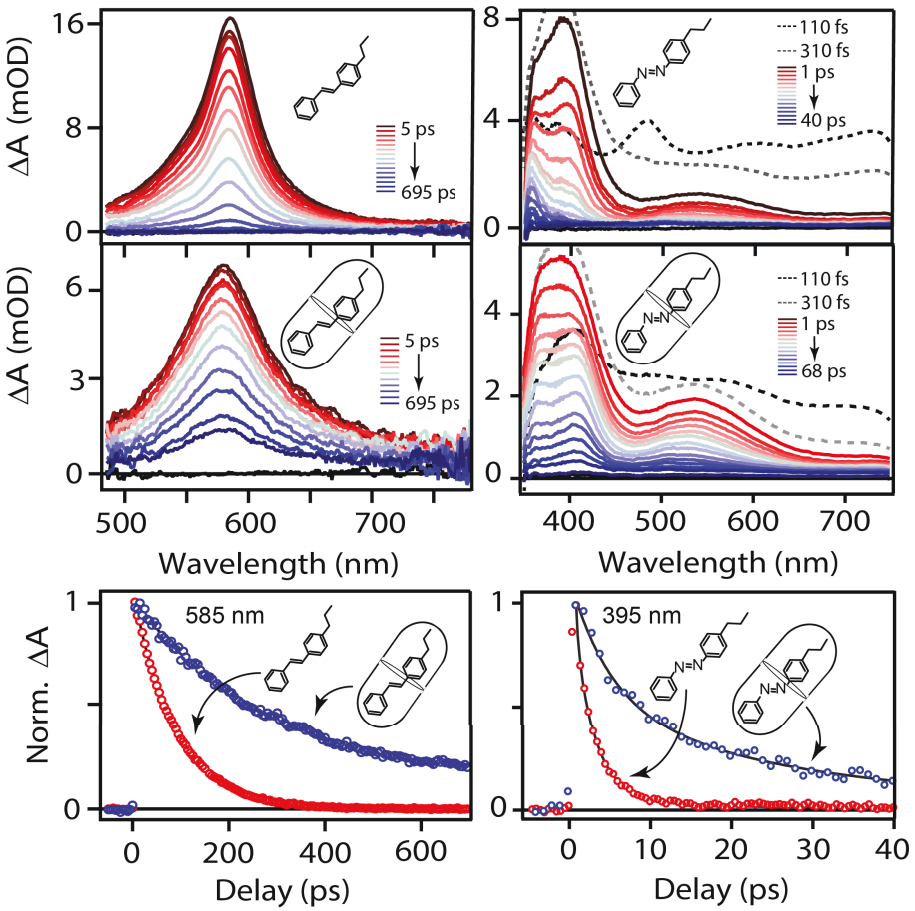

Figure 2: Evolution of the TA spectra of 4PrSt (left side) and 4PrAz (right side). Top and middle panels show the spectra in cyclohexane and in the OA_2 capsules, respectively. The lower panels compare the decay of the normalized TA signals in the two environments, with the lines showing fits to the data using the models described in the text.

Similar to unsubstituted stilbene,[36,37] the TA spectrum of 4PrSt in cyclohexane has a strong S_1 excited-state absorption (ESA) band centered near 580 nm that shifts and narrows slightly on a timescale of 1.3 ± 0.3 ps due to structural relaxation and vibrational cooling (figure S6), and then decays with a single exponential lifetime of 86 ± 3 ps. The TA spectrum of encapsulated 4PrSt (4PrSt@OA_2) is similar to the solvated compound, except for a slight blue-shift and broadening of the ESA band, and a significantly longer excited-state lifetime of 384 ± 4 ps. The broadening of the ESA band in the capsule suggests either a more distorted structure or a broader distribution of structures compared with solution, similar to what we

observe in the ground-state spectrum and simulations.

The isomerization mechanism for stilbene has been well-studied in solution.[29,37,38] After $\pi\pi^*$ excitation to S_1, stilbene molecules cross a small barrier along the torsional rotation coordinate before reaching a perpendicular geometry, where there is a conical intersection (CI) that brings the molecule back to the ground electronic state.[39] The excited-state lifetime for many stilbene derivatives is on the order of tens of ps, depending on the solvent, and has been successfully described in terms of either solvent viscosity inhibiting the relative rotation of the phenyl rings, or with a solvent stabilization model where the polarity of the solvent affects the activation energy to reach the CI at perpendicular geometry.[29,40] Either way, the longer excited-state lifetime for 4PrSt@OA_2 is most likely due to restricted rotation around the C=C bond inside the capsule.

Passage through the CI determines the branching between *trans* and *cis* isomers when molecules return to the ground state. For stilbene in solution, this branching leads to nearly equal populations of the two isomers. Importantly, the quantum yield ($\Phi_{t\rightarrow c}$) for *trans*→*cis* isomerization of stilbene is relatively insensitive to the identity of the solvent,[36,38,41] indicating that solvation does not directly affect the topology of the S_1-S_0 conical intersection. However, we find that encapsulation in OA_2 decreases $\Phi_{t\rightarrow c}$ by nearly half, from $42 \pm 6\%$ in cyclohexane to $24 \pm 6\%$ in the capsule. A very modest increase of the fluorescence yield, from 5% to 6%, reflects the extended excited-state lifetime in the capsule, but does not account for the significantly lower quantum yield for isomerization. Instead, the lower isomerization yield suggests that confinement directly impacts the dynamics through the CI, possibly by altering the topology of the CI itself. For example, the encapsulated molecule may pass through a CI (or a region of the conical seam) that is shifted toward the *trans* geometry due to destabilization of the perpendicular structure.

The excited-state lifetime of 4PrAz is much shorter than 4PrSt, with the former also following a more complex pathway that requires fits to the data with at least four time constants in solution and five in the capsule. One key difference between the two compounds

is that excitation at 320 nm accesses the $S_2(\pi\pi^*)$ state of 4PrAz, which rapidly relaxes to the lower-lying $S_1(n\pi^*)$ electronic state. The ESA spectrum of S_2, which is evident only within the first ∼300 fs of the TA spectra for 4PrAz and 4PrAz@OA_2 (dashed lines in figure 2), extends across the entire probe range, with broad bands centered near 490, 600 and 710 nm. Similar to previous reports for unsubstituted azobenzene, the S_2 absorption is rapidly replaced by the S_1 absorption bands near 400 and 530 nm (figure S7 of the SI), which then decay within a few ps.[42]

In contrast with stilbene, the isomerization mechanism for azobenzene derivatives remains controversial, because of the competing pathways involving torsional rotation and in-plane inversion at one (or both) of the nitrogen atoms. The limit of rotational isomerization involves torsion around the N=N bond to reach a conical intersection with the ground-state at perpendicular geometry, similar to stilbene; however, azobenzene can also isomerize through an inversion pathway via rehybridization of the non-bonding electrons and in-plane bending of a phenyl ring along the Ph-N=N coordinate.[43–47]

Based on the relative electronic structures of the first two excited states of azobenzene, early studies suggested that $n \rightarrow \pi^*$ excitation to S_1 would result in primarily an inversion mechanism, whereas $\pi \rightarrow \pi^*$ excitation to S_2 would result in primarily a rotational mechanism analogous to stilbene photoisomerization. However, more recent experimental and theoretical work indicates that a simple, single-configuration view of the excited states does not adequately describe the isomerization dynamics of azobenzene, but rather the dynamics involve an "inversion-assisted rotation" mechanism that requires concerted motion along both coordinates due to mixing of the $n\pi^*$ and $\pi\pi^*$ states along the reaction path.

The situation is further complicated for excitation to the higher-energy $\pi\pi^*$ state, because additional isomerization and relaxation channels are available in the vibrationally excited S_1 state after internal conversion from S_2.[42] Very briefly, the lowest-energy isomerization pathway on S_1 begins with in-plane motion along the inversion coordinate, and then involves some degree of rotation to access a conical seam that returns the system to the ground state.

Different regions of the conical seam involving a larger degree of rotation are available at higher energy. (See the SI of reference 42 for an excellent historical review of the azobenzene isomerization mechanism.)

The top panel of Figure 3 shows a simplified schematic representation of the emerging mechanism for azobenzene photoisomerization following $\pi \rightarrow \pi^*$ excitation to S_2,[42,48] including the lifetimes that we extract from global fits to the TA data for 4PrAz in cyclohexane. The fastest timescale of ∼50 fs is due to relaxation from S_2 to S_1, followed by ∼260 fs relaxation of the "hot" S_1 state. While a portion of the molecules relax into a minimum-energy geometry on the S_1 surface, a large fraction of the "hot" molecules reach the ground state on a timescale that competes with vibrational relaxation in S_1.[49] The result is a roughly biexponential decay of the ESA signal on timescales of ∼0.26 ps for the "hot" reacting molecules and ∼2.4 ps for molecules that relax on S_1 before overcoming the small barrier along the minimum energy path. Molecules return to the ground state through a CI that determines the relative branching between *cis* and *trans* isomers. Molecules that return to the *trans* structure in the ground state contribute a transient absorption feature below 400 nm that decays on a timescale of ∼ 10 ps due to vibrational relaxation and cooling in S_0.[48–51] The ground-state of the *cis* isomer and the relaxed S_0 state of the *trans* isomer do not contribute to the absorption in our probe window.

We model the evolution of the TA spectrum of 4PrAz in cyclohexane based on the above kinetic mechanism. Our fits to the data restrict the relative amplitudes at each wavelength according to the kinetic model in order to extract the species-associated spectra (SAS) in the top panel of figure 4. The SAS represent distinct populations of 4PrAz along the reaction path, including molecules in the initially excited S_2 state, the hot and relaxed S_1 states (S_1^* and S_1, respectively), and the vibrationally hot ground state of the *trans* isomer (S_0^*). We use a fixed time constant of 50 fs for the decay of S_2 based on earlier work,[42] and determine the other time constants from best fits to the data. The negative feature near 400 nm in the spectrum associated with S_2 is due to stimulated emission, consistent with the strong S_2

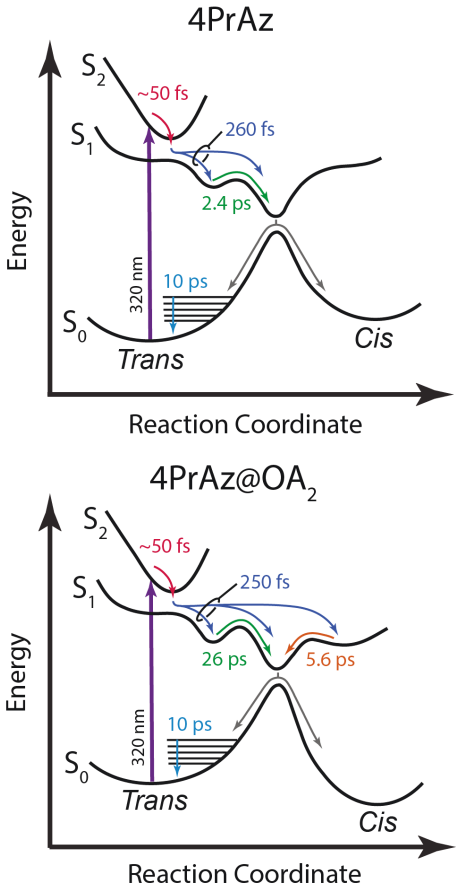

Figure 3: Cartoon illustration of the potential energy surfaces for 4PrAz and 4PrAz@OA_2. Arrows indicate reaction path following $\pi \rightarrow \pi^*$ excitation. Lifetimes are from global fits to the data using the kinetic model described in the text and in figure 4.

fluorescence band of azobenzene at that wavelength.[45]

The spectra obtained from the fits support the proposed mechanism from above. In particular, the spectra for S_1 and S_1^* are very similar, with the latter characterized by additional broadening, which is typical for highly vibrationally excited molecules.[36,52] The spectrum also shifts to slightly longer (rather than shorter) wavelength for the relaxed S_1, which indicates some structural relaxation in addition to vibrational cooling in the excited-state. In other words, the relaxation of S_1^* leads to a narrowing and shifting of the ESA band, in addition to a decrease of intensity in the overall TA signal on the same time scale due to the competing reaction channel directly from S_1^* to the ground state. The fits indicate that $\sim 60\%$ of the "hot" molecules relax directly to the ground electronic state in cyclohexane.

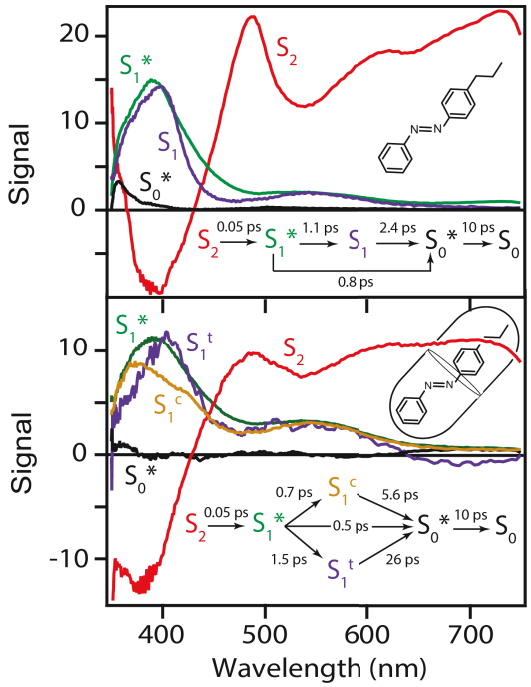

Figure 4: Species associated spectra (SAS) from global fits to the TA spectra for 4PrAz in cyclohexane (top) and 4PrAz@OA_2 (bottom). The kinetic models are shown as insets, and match the schematic diagrams in figure 3. See the SI for plots of the time-dependent populations from the global fits.

The TA spectrum of confined 4PrAz (4PrAz@OA_2) is similar to the spectrum in solution, except for a few notable differences, including different relative intensities of the ESA bands near 400 and 530 nm, slight broadening of the bands, and a significantly longer excited-state lifetime. The differences between the two environments in many ways mirror the results for 4PrSt. However, global fits to the data for 4PrAz@OA_2 require at least five exponential time constants, compared with only four in solution. The extra lifetime is associated with a unique feature in the TA spectrum, and indicates that there are two distinct excited-state species in the capsule. Figure S9 of the SI shows the decay-associated spectra (DAS) for both environments.

Using the mechanism for azobenzene in solution as a starting point, we modeled the evolution of the TA spectrum of 4PrAz@OA_2 using several different kinetic schemes. Each scheme includes an additional excited-state species, S_1', to account for the extra feature in the DAS. Our modeling suggests that a simple sequential relaxation mechanism is not sufficient

to recover the evolution of the TA spectrum at all wavelengths. Only a mechanism that includes parallel kinetics for the two distinct excited-state species (both originating from S_1^*) gives a reasonable fit to the data. The successful model and resulting SAS are represented in the bottom panel of figure 4. The lifetimes from the global fits are summarized in Table S2 of the SI.

The spectrum associated with the S_2 state of 4PrAz@OA_2 is similar to the S_2 spectrum in solution, except for significant broadening of the ESA band near 490 nm that probably reflects a distorted geometry in the confined environment of the capsule. Relaxation to S_1^* occurs on a similar sub-100 fs time scale (we fix this time constant at 50 fs in our fits based on recent results from Nenov, *et al.*[42]), and both the spectrum and relaxation time of S_1^* that we recover from the fits in the capsule are similar to those in solution, indicating that the dynamics at very early delay times are relatively insensitive to confinement.[11] However, a distinctive feature of the dynamics of 4PrAz@OA_2 is the relaxation of S_1^* into two different excited-state species, in addition to direct relaxation to the ground state. The two species have lifetimes of 5.6 ± 1.1 and 26 ± 2 ps.

Importantly, one of the spectra that we recover from the global fits has an ESA band with a maximum near 380 nm and a pronounced shoulder near 410 nm. This distinctive feature closely resembles the excited-state spectrum that was previously reported following $\pi \rightarrow \pi^*$ excitation of unsubstituted *cis*-azobenzene (Az) in solution.[48] In separate TA measurements, shown in Figure S15 of the SI, we observe a very similar ESA band for direct $n \rightarrow \pi^*$ excitation of encapsulated *cis*-Az. The distinctive spectrum and 1.3 ps lifetime for *cis*-Az@OA_2 are identical to the S_1' feature that we obtain from global fits following $\pi \rightarrow \pi^*$ excitation of unsubstituted *trans*-Az@OA_2, indicating a common excited-state species following excitation of either ground-state isomer in the capsule. Although the timescales are slightly different for Az@OA_2 and 4PrAz@OA_2 (1.3 *vs.* 5.6 ps), the S_1' spectrum is nearly the same for both compounds. Therefore, we assign the two excited-state species of 4PrAz@OA_2 as the relaxed S_1 states of the *cis* and *trans* isomers, S_1^{cis} and S_1^{trans}, respectively. In stark contrast with

solution, this observation indicates that the confined environment allows 4PrAz to access the *cis* structure directly from the excited state of the *trans* isomer. This new excited-state isomerization pathway to S_1^{cis} is made possible by destabilization of the longer *trans* structure in the capsule, and probably leads to a distorted structure compared with the *cis* excited state in solution.

The results for similarly sized 4PrSt show that the rotation channel is restricted in the capsule, therefore the excited-state isomerization of 4PrAz to S_1^{cis} must follow a path primarily along the inversion coordinate. The important role of inversion in the isomerization of 4PrAz@OA_2 is further supported by an *increase* of the quantum yield $\Phi_{t\rightarrow c}$ from 12±3% in solution to 17±4% in the capsule, in contrast with the significant decrease of $\Phi_{t\rightarrow c}$ for 4PrSt. The larger quantum yield for isomerization of 4PrAz@OA_2 is a direct result of steric crowding inside the capsule that favors the *cis* geometry. In solution, the overall quantum yield for azobenzene depends on the initial excitation energy, with a photoisomerization yield for $\pi \rightarrow \pi^*$ excitation of unsubstituted azobenzene that is about half of the yield for $n \rightarrow \pi^*$ excitation of the same molecule at longer wavelengths.[53] The wavelength-dependence of $\Phi_{t\rightarrow c}$ in solution was attributed to a preference for the *trans* structure when molecules pass through a CI at higher energy. In other words, regions of the conical seam that are accessible at higher energy have a topology that increasingly favors a return to the *trans* structure in the ground electronic state.

Encapsulation restricts the motions available to an isomerizing molecule, and therefore drives the reaction through different regions of the conical seam compared with solution. The fits indicate that roughly half of the "hot" S_1^* molecules relax directly to the ground electronic state within the first few hundred fs, whereas molecules that remain in the excited state have a roughly 2:1 preference for the formation of S_1^{cis} over S_1^{trans}. Although we are unable to directly measure the quantum yields for each of the three pathways individually, there is likely to be a higher yield of the *cis* product from the *cis* excited-state. However, the modest increase of the overall quantum yield to only ∼17% in the capsule suggests that

both "hot" S_1^* and the *trans* excited state preferentially return to the *trans* structure in S_0.

We extract lifetimes from the global fits of 5.6 ps for S_1^{cis} and 26 ps for S_1^{trans}. The excited-state lifetime of S_1^{trans} is ∼10 times longer in the capsule than in solution, indicating that the confined environment has a significant impact on the isomerization dynamics of 4PrAz, probably due to trapping the molecule in a distorted (*i.e.* non-planar) structure. We note that the ESA band of this species is red-shifted compared with solution (and with S_1^*), which may be a signature of the twisted structure in the capsule. A twisted geometry of S_1^{trans} would inhibit photoisomerization of 4PrAz@OA_2 by restricting in-plane motion along the inversion coordinate, which was recently shown to be the initial motion along the minimum energy path of S_1 in solution.[42] Consistent with this assignment of the longer-lived ESA band as S_1^{trans}, direct excitation to the $S_1(n\pi^*)$ state of unsubstituted *trans*-azobenzene (figure S15) reveals a similar ten-fold increase of the exited-state lifetime inside the OA_2 capsule.

The new pathway to access S_1^{cis} following excitation to the $S_2(\pi\pi^*)$ state of 4PrAz@OA_2 is only available from the "hot" S_1^* excited state, and is made possible by the destabilization of the *trans* structure in the capsule. We note that the quantum yield does not increase for other alkyl-substituted azobenzenes, as we will report elsewhere. The unique increase of $\Phi_{t\rightarrow c}$ for 4PrAz@OA_2 is due to crowding in the capsule by the propyl substituent on one phenyl ring, combined with the flexibility of the unsubstituted phenyl ring to reorient within the capsule. We are currently studying the excited-state dynamics for a series of alkyl-substituted azobenzene compounds to further elucidate the role that crowding in the capsule plays in determining the excited-state isomerization.

In summary, ultrafast spectroscopy reveals fundamentally different excited-state dynamics for 4PrSt and 4PrAz inside the cavity of a supramolecular organic cavitand than we observe for the same compounds in solution. The encapsulated molecules have longer excited-state lifetimes due to stabilization of distorted, nonplanar excited-state structures. While both 4PrSt and 4PrAz prefer the *cis* isomer in the capsule, only 4PrAz shows an increase of the quantum yield for *trans*→*cis* photoisomerization. Specifically, confinement restricts out-

of-plane rotation of the phenyl rings, and therefore inhibits the photoisomerization of 4PrSt, whereas the inversion channel of azobenzene leads to a new excited-state isomerization channel for encapsulated 4PrAz that does not exist in solution. The new channel leading to the *cis* excited state following excitation of the *trans* isomer represents a fundamentally different behavior than has been observed before, and confirms the important role of inversion in the isomerization of azobenzene.

Experimental Methods

The compounds OA, 4PrSt, and 4PrAz were synthesized and purified as previously reported.[31,33] Samples consist of 1 mM solutions of 4PrSt or 4PrAz in cyclohexane, or ~ 0.5 mM aqueous solutions of the encapsulated compounds. We make the self-assembled 4PrSt@OA_2 and 4PrAz@OA_2 complexes by sonicating 2 eq. of OA with 1 eq. of stilbene or azobenzene derivative for 30 min in water. All samples are in a 1 mm quartz cuvette.

The transient absorption (TA) and quantum yield (QY) measurements use the modified output of a regeneratively amplified Ti:sapphire laser (Legend Elite, Coherent) operating at 1 kHz. An optical parametric amplifier (OPA) with two stages of nonlinear frequency conversion (TOPAS) produces 320 nm pump pulses for both measurements. For the TA measurements, the pump beam passes though a synchronized chopper to block every other pulse for active background subtraction, a zero-order $\lambda/2$ waveplate rotates the polarization for parallel and perpendicular orientation with respect to the probe, and a CaF_2 prism pair compresses the pump pulses for a pump-probe time resolution of $\sim$100 fs. We attenuate and focus the pump beam to $\sim$ 120 nJ/pulse and a diameter of $\sim 200\mu m$ at the sample, which is continuously translating in order to avoid accumulation of photoproduct in the focal volume. We generate broadband probe pulses in the range of 340-990 nm by focusing a small amount of the 1200 nm signal from a second, home-built OPA into a circularly translating CaF_2 crystal for white-light continuum generation. A pair of parabolic mirrors collimate

and focus the probe into the sample, where it intersects the pump at a small angle and variable time delay. After passing though the sample, a prism disperses the probe light onto a 256-element photodiode array for shot-to-shot detection.

Each TA measurement is an average of three consecutive scans with 10^3 laser pulses per time delay. We use custom code written in Igor Pro for global fits to the TA data using either a sum of exponentials to obtain the decay-associated spectra (DAS), or a kinetic model to obtain species-associated spectra (SAS). The kinetic models are described in the text, with additional details from the global fits provided in the SI.

We measure *trans* $\rightarrow$ *cis* photoisomerization quantum yields ($\Phi_{t\rightarrow c}$) by measuring the change in transmission of UV laser pulses through a static sample as a function of time.[36] For both compounds, the *trans* isomer has appreciable absorption at the excitation wavelength, but *cis* does not; therefore the decrease in transmission through the sample reveals the number of molecules that isomerize. We obtain the quantum yield from the ratio of the conversion rate to the excitation rate (*i.e.* the relative change of transmission over time compared with the absolute transmission of 320 nm pulses). In order to account for small fluctuations of the laser intensity, we split the attenuated pump light into signal and reference beams with a 50% beam splitter, and then pass the former through the sample with a diameter of 1.5 mm and an incident energy of 2.5 nJ/pulse. We measure the pulse energies of the transmitted signal and reference beams using identical integrating photodiodes at 1 kHz.

Supporting Information

The supplemental information (SI) includes structures of OA and the 4PrSt@OA_2 complex, NMR spectra confirming the encapsulation of the *trans* isomers of each compound, anisotropy decay measurements, and additional transient absorption spectra and analysis.

Acknowledgements

This material is based upon work supported by the National Science Foundation under grant number CHE-1807729 (VR) and Career Award CHE-1151555 (CGE). The authors thank Prof. Rajeev Prabhakar and Gaurav Sharma at the University of Miami for providing the simulated structures of stilbene derivatives inside OA_2 capsules.

References

(1) Ernst, O. P.; Lodowski, D. T.; Elstner, M.; Hegemann, P.; Brown, L. S.; Kandori, H. Microbial and animal rhodopsins: Structures, functions, and molecular mechanisms. *Chem. Rev.* **2014**, *114*, 126–163.

(2) Vengris, M.; van der Horst, M.; Zgrablic, G.; van Stokkum, I.; Haacke, S.; Chergui, M.; Hellingwerf, K.; van Grondelle, R.; Larsen, D. Contrasting the excited-state dynamics of the photoactive yellow protein chromophore: Protein versus solvent environments. *Biophys. J.* **2004**, *87*, 1848–1857.

(3) Kukura, P.; McCamant, D.; Yoon, S.; Wandschneider, D.; Mathies, R. Structural observation of the primary isomerization in vision with femtosecond-stimulated Raman. *Science* **2005**, *310*, 1006–1009.

(4) Polli, D.; Altoe, P.; Weingart, O.; Spillane, K. M.; Manzoni, C.; Brida, D.; Tomasello, G.; Orlandi, G.; Kukura, P.; Mathies, R. A. et al. Conical intersection dynamics of the primary photoisomerization event in vision. *Nature* **2010**, *467*, 440–443.

(5) Gozem, S.; Luk, H. L.; Schapiro, I.; Olivucci, M. Theory and simulation of the ultrafast double-bond isomerization of biological chromophores. *Chem. Rev.* **2017**, *117*, 13502–13565.

(6) Duveneck, G.; Sitzmann, E.; Eisenthal, K.; Turro, N. Picosecond laser studies on photochemical-reactions in restricted environments: The photoisomerization of *trans*-stilbene complexed to cyclodextrins. *J. Phys. Chem.* **1989**, *93*, 7166–7170.

(7) Takei, M.; Yui, H.; Hirose, Y.; Sawada, T. Femtosecond time-resolved spectroscopy of photoisomerization of methyl orange in cyclodextrins. *J. Phys. Chem. A* **2001**, *105*, 11395–11399.

(8) Liu, R. S. H.; Hammond, G. S. Reflection on medium effects on photochemical reactivity. *Acc. Chem. Res.* **2005**, *38*, 396–403.

(9) Muraoka, T.; Kinbara, K.; Aida, T. Mechanical twisting of a guest by a photoresponsive host. *Nature* **2006**, *440*, 512.

(10) Ramamurthy, V. Photochemistry within a water-soluble organic capsule. *Acc. Chem. Res.* **2015**, *48*, 2904–2917.

(11) Bahrenburg, J.; Renth, F.; Temps, F.; Plamper, F.; Richtering, W. Femtosecond spectroscopy reveals huge differences in the photoisomerisation dynamics between azobenzenes linked to polymers and azobenzenes in solution. *Phys. Chem. Chem. Phys.* **2014**, *16*, 11549–11554.

(12) Otte, M. Size-selective molecular flasks. *ACS Catal.* **2016**, *6*, 6491–6510.

(13) Grimmelsmann, L.; Khah, A. M.; Spies, C.; Haettig, C.; Nuernberger, P. Ultrafast dynamics of a triazene: Excited-state pathways and the impact of binding to the minor groove of DNA and further biomolecular systems. *J. Phys. Chem. Lett.* **2017**, *8*, 1986–1992.

(14) Ramamurthy, V.; Parthasarathy, A. Chemistry in restricted spaces: Select photodimerizations in cages, cavities, and capsules. *Isr. J. Chem.* **2011**, *51*, 817–829.

(15) Parthasarathy, A.; Ramamurthy, V. Water-soluble octa acid capsule as a reaction container: Templated photodimerization of indene in water. *J. Photochem. Photobiol., A* **2016**, *317*, 132–139.

(16) Valentini, A.; Rivero, D.; Zapata, F.; Garcia-Iriepa, C.; Marazzi, M.; Palmeiro, R.; Galvan, I. F.; Sampedro, D.; Olivucci, M.; Manuel Frutos, L. Optomechanical control of quantum yield in *trans-cis* ultrafast photoisomerization of a retinal chromophore model. *Angew. Chem., Int. Ed.* **2017**, *56*, 3842–3846.

(17) Beharry, A. A.; Woolley, G. A. Azobenzene photoswitches for biomolecules. *Chem. Soc. Rev.* **2011**, *40*, 4422–4437.

(18) Dugave, C.; Demange, L. *cis−trans* isomerization of organic molecules and biomolecules: Implications and applications. *Chem. Rev.* **2003**, *103*, 2475–2532.

(19) Banghart, M.; Mourot, A.; Fortin, D.; Yao, J.; Kramer, R.; Trauner, D. Photochromic blockers of voltage-gated potassium channels. *Angew. Chem., Int. Ed.* **2009**, *48*, 9097–9101.

(20) Kim, Y.; Phillips, J. A.; Liu, H.; Kang, H.; Tan, W. Using photons to manipulate enzyme inhibition by an azobenzene-modified nucleic acid probe. *Proc. Natl. Acad. Sci.* **2009**, *106*, 6489–6494.

(21) Wang, J.; Liu, H.-B.; Ha, C.-S. Zinc-supported azobenzene derivative-based colorimetric fluorescent 'turn-on' sensing of bovine serum albumin. *Tetrahedron* **2009**, *65*, 9686–9689.

(22) Banghart, M.; Borges, K.; Isacoff, E.; Trauner, D.; Kramer, R. H. Light-activated ion channels for remote control of neuronal firing. *Nat. Neurosci.* **2004**, *7*, 1381.

(23) Norikane, Y.; Tamaoki, N. Light-driven molecular hinge: A new molecular machine

showing a light-intensity-dependent photoresponse that utilizes the *trans*−*cis* isomerization of azobenzene. *Org. Lett.* **2004**, *6*, 2595–2598.

(24) Murakami, H.; Kawabuchi, A.; Kotoo, K.; Kunitake, M.; Nakashima, N. A light-driven molecular shuttle based on a rotaxane. *J. Am. Chem. Soc.* **1997**, *119*, 7605–7606.

(25) Wen, Y.; Yi, W.; Meng, L.; Feng, M.; Jiang, G.; Yuan, W.; Zhang, Y.; Gao, H.; Jiang, L.; Song, Y. Photochemical-controlled switching based on azobenzene monolayer modified silicon (111) surface. *J. Phys. Chem. B* **2005**, *109*, 14465–14468.

(26) Kakiage, K.; Yamamura, M.; Ido, E.; Kyomen, T.; Unno, M.; Hanaya, M. Reactivity of alkoxysilyl compounds: Chemical surface modification of nano-porous alumina membrane using alkoxysilylazobenzenes. *Appl. Organomet. Chem.* **2011**, *25*, 98–104.

(27) Masahide, I.; Kenji, H.; Shun-ichi, K.; Toyohiko, Y. Holographic recording on azobenzene functionalized polymer film. *Jpn. J. Appl. Phys.* **2004**, *43*, 4968.

(28) Jiang, X. L.; Li, L.; Kumar, J.; Kim, D. Y.; Tripathy, S. K. Unusual polarization dependent optical erasure of surface relief gratings on azobenzene polymer films. *Appl. Phys. Lett.* **1998**, *72*, 2502–2504.

(29) Waldeck, D. Photoisomerization dynamics of stilbenes. *Chem. Rev.* **1991**, *91*, 415–436.

(30) Bandara, H. M. D.; Burdette, S. C. Photoisomerization in different classes of azobenzene. *Chem. Soc. Rev.* **2012**, *41*, 1809–1825.

(31) Parthasarathy, A.; Kaanumalle, L. S.; Ramamurthy, V. Controlling photochemical geometric isomerization of a stilbene and dimerization of a styrene using a confined reaction cavity in water. *Org. Lett.* **2007**, *9*, 5059–5062.

(32) Samanta, S. R.; Parthasarathy, A.; Ramamurthy, V. Supramolecular control during triplet sensitized geometric isomerization of stilbenes encapsulated in a water soluble organic capsule. *Photochem. Photobiol. Sci.* **2012**, *11*, 1652–1660.

(33) Mohan Raj, A.; Ramamurthy, V. Volume conserving geometric isomerization of encapsulated azobenzenes in ground and excited states and as radical ion. *Org. Lett.* **2017**, *19*, 6116–6119.

(34) Porel, M.; Jockusch, S.; Parthasarathy, A.; Rao, V. J.; Turro, N. J.; Ramamurthy, V. Photoinduced electron transfer between a donor and an acceptor separated by a capsular wall. *Chem. Comm.* **2012**, *48*, 2710–2712.

(35) Gibb, C. L. D.; Gibb, B. C. Well-defined, organic nanoenvironments in water: The hydrophobic effect drives a capsular assembly. *J. Am. Chem. Soc.* **2004**, *126*, 11408–11409.

(36) Houk, A. L.; Zheldakov, I. L.; Tommey, T. A.; Elles, C. G. Two-photon excitation of *trans*-stilbene: Spectroscopy and dynamics of electronically excited states above S_1. *J. Phys. Chem. B* **2015**, *119*, 9335–9344.

(37) Kovalenko, S. A.; Dobryakov, A. L.; Ioffe, I.; Ernsting, N. P. Evidence for the phantom state in photoinduced *cis-trans* isomerization of stilbene. *Chem. Phys. Lett.* **2010**, *493*, 255–258.

(38) Hochstrasser, R. Picosecond processes in the isomerism of stilbenes. *Pure Appl. Chem.* **1980**, *52*, 2683–2691.

(39) Levine, B. G.; Martinez, T. J. Isomerization through conical intersections. *Annu. Rev. Phys. Chem.* **2007**, *58*, 613–634.

(40) Ioffe, I. N.; Quick, M.; Quick, M. T.; Dobryakov, A. L.; Richter, C.; Granovsky, A. A.; Berndt, F.; Mahrwald, R.; Ernsting, N. P.; Kovalenko, S. A. Tuning stilbene photochemistry by fluorination: State reordering leads to sudden polarization near the Franck–Condon region. *J. Am. Chem. Soc.* **2017**, *139*, 15265–15274, PMID: 28985461.

(41) Hammond, G. S.; Saltiel, J.; Lamola, A. A.; Turro, N. J.; Bradshaw, J. S.; Cowan, D. O.; Counsell, R. C.; Vogt, V.; Dalton, C. Mechanisms of photochemical reactions in solution. XXII. Photochemical *cis-trans* isomerization. *J. Am. Chem. Soc.* **1964**, *86*, 3197–3217.

(42) Nenov, A.; Borrego-Varillas, R.; Oriana, A.; Ganzer, L.; Segatta, F.; Conti, I.; Segarra-Marti, J.; Omachi, J.; Dapor, M.; Taioli, S. et al. UV-light-induced vibrational coherences: The key to understand Kasha rule violation in *trans*-azobenzene. *J. Phys. Chem. Lett.* **2018**, *9*, 1534–1541.

(43) Wei-Guang Diau, E. A new *trans*-to-*cis* photoisomerization mechanism of azobenzene on the $S_1(n,\pi^*)$ surface. *J. Phys. Chem. A* **2004**, *108*, 950–956.

(44) Lednev, I. K.; Ye, T.-Q.; Hester, R. E.; Moore, J. N. Femtosecond time-resolved UV−visible absorption spectroscopy of *trans*-azobenzene in solution. *J. Phys. Chem.* **1996**, *100*, 13338–13341.

(45) Fujino, T.; Arzhantsev, S. Y.; Tahara, T. Femtosecond time-resolved fluorescence study of photoisomerization of *trans*-azobenzene. *J. Phys. Chem. A* **2001**, *105*, 8123–8129.

(46) Stuart, C. M.; Frontiera, R. R.; Mathies, R. A. Excited-state structure and dynamics of *cis*- and *trans*-azobenzene from resonance Raman intensity analysis. *J. Phys. Chem. A* **2007**, *111*, 12072–12080.

(47) Fujino, T.; Tahara, T. Picosecond time-resolved Raman study of *trans*-azobenzene. *J. Phys. Chem. A* **2000**, *104*, 4203–4210.

(48) Satzger, H.; Root, C.; Braun, M. Excited-state dynamics of *trans*- and *cis*-azobenzene after UV excitation in the $\pi\pi^*$ band. *J. Phys. Chem. A* **2004**, *108*, 6265–6271.

(49) Quick, M.; Dobryakov, A. L.; Gerecke, M.; Richter, C.; Berndt, F.; Ioffe, I. N.; Granovsky, A. A.; Mahrwald, R.; Ernsting, N. P.; Kovalenko, S. A. Photoisomerization

dynamics and pathways of *trans*- and *cis*-azobenzene in solution from broadband femtosecond spectroscopies and calculations. *J. Phys. Chem. B* **2014**, *118*, 8756–8771.

(50) Lednev, I. K.; Ye, T. Q.; Matousek, P.; Towrie, M.; Foggi, P.; Neuwahl, F. V. R.; Umapathy, S.; Hester, R. E.; Moore, J. N. Femtosecond time-resolved UV-visible absorption spectroscopy of trans-azobenzene: dependence on excitation wavelength. *Chem. Phys. Lett.* **1998**, *290*, 68–74.

(51) Tatsuya, F.; Yu., A. S.; Tahei, T. Femtosecond/picosecond time-resolved spectroscopy of *trans*-azobenzene: Isomerization mechanism following $S_2(\pi\pi*)\leftarrow S_0$ photoexcitation. *Bull. Chem. Soc. Jpn.* **2002**, *75*, 1031–1040.

(52) Kovalenko, S. A.; Schanz, R.; Hennig, H.; Ernsting, N. P. Cooling dynamics of an optically excited molecular probe in solution from femtosecond broadband transient absorption spectroscopy. *J. Chem. Phys.* **2001**, *115*, 3256–3273.

(53) Lednev, I. K.; Ye, T.-Q.; Abbott, L. C.; Hester, R. E.; Moore, J. N. Photoisomerization of a capped azobenzene in solution probed by ultrafast time-resolved electronic absorption spectroscopy. *J. Phys. Chem. A* **1998**, *102*, 9161–9166.